Research Square

Preprints are preliminary reports that have not undergone peer review.
They should not be considered conclusive, used to inform clinical practice,
or referenced by the media as validated information.

Long non coding RNA CCAT2 enhances the proliferation, migration, invasion and drug-resistances of non-small lung cancer *via* activating the miR-204-3p-suppresed IGFBP2/AKT/Bcl_2 pathway

Zheng Wang
Department of thoracic surgery, Cancer Hospital of China Medicine University, Liaoning Cancer Hospital & Insititute.

Rongjie Yang
Department of thoracic surgery, Cancer Hospital of China Medicine University, Liaoning Cancer Hospital & Institute

Yu Liu
Department of thoracic surgery, Cancer Hospital of China Medicine University, Liaoning Cancer Hospital & Institute.

Yanfeng Huang (yanfenghuangyfg@aliyun.com)
Department of thoracic surgery, Cancer Hospital of China Medical University, Liaoning Cancer Hospital & Institute. Shenyang 110042 https://orcid.org/0000-0002-4576-0105

Primary research

Keywords: non-small cell lung cancer, colon cancer-associated transcript 2, IGF-binding protein, miR-204-3p, drug-resistance

Posted Date: June 17th, 2020

DOI: https://doi.org/10.21203/rs.3.rs-25814/v2

License: This work is licensed under a Creative Commons Attribution 4.0 International License.
Read Full License

Abstract

Background: To date, the treatment efficacy of NSCLC remains unsatisfactory mainly ascribed to the rapid progress, high rate of metastasis, and emerged drug-resistance. It has been demonstrated that aberrant expression of long non coding RNA colon cancer-associated transcript 2 (CCAT2) was closely related to tumorigenesis and development of drug-resistance of many cancer types. The present study was aimed to thoroughly investigate the effect of CCAT2 in the progress of NSCLC and the underlying mechanisms, so that provide valuable theoretical basis for efficient treatment of NSCLC.

Methods: The expressions of CCAT2 were determined using the RT-qPCR experiment. Its target genes and downstream molecules were respectively evaluated by Western-blot assay and RT-qPCR experiment. Cell growth of NSCLC cells was investigated using the CCK-8 kit. The effect of CCAT2 on the progress of NSCLC and the underlying mechanisms *in vivo* was determined on the NSCLC-bearing mice models.

Results: Higher expression of CCAT2 was detected in the lung cancer tissues and cells than the normal ones. Moreover, it was revealed that aberrant expression of CCAT2 in lung cancer signally contributed to proliferation, invasion, and migration of cancer cells and the progress of tumor tissues. Additionally, high level of CCAT2 dramatically down-regulated the cytotoxicity of cisplatin (DDP) to NSCLC cells and tissues by upregulation of the drug-resistance related proteins. Mechanisms studies displayed that upregulation of CCAT2 markedly decreased the miR-204-3p while contrary result was obtained when down-regulated the CCAT2 level. We further demonstrated that down-regulation of miR-204-3p level signally enhanced the activity of the insulin-like growth factor (IGF) signaling pathway.

Conclusions: The CCAT2 promoted the progress and drug-resistance of NSCLC thorough activation of the miR-204-3p suppressed IGFBP2/AKT/Bcl2 pathway, and may provide theoretical basis for improvement of therapy of NSCLC.

Background

As one of the most commonly diagnosed cancer types, lung cancer has the highest mortality rates in worldwide [1,2]. The NSCLC is the most malignant lung cancer type with rapid and progress and metastasis [3]. Most of NSCLCs were diagnosed at an advanced stage, which paved a rough road for the treatment [4]. The limited effectiveness of current treatments leads to a low 5-year survival rate and an extremely poor prognosis for the NSCLC [5,6]. Additionally, majority of NSCLC patients inevitably developed the multidrug resistance within a year even they were initially sensitive enough to the treatment of chemotherapy [7-9]. Thoroughly understanding the molecule mechanisms underlying tumorigenesis, progress and drug-resistance is therefore urgently required for enhanced the treatment effect of NSCLC.

Long non-coding RNA (LncRNA), belongs to ncRNAs, represents a class of transcripts with a length of >200 nucleotides [10]. It was previously revealed that abnormal expression of lncRNAs was always correlated to tumorigenesis, tumor progress and tumor metastasis [11]. The levels of CCAT2 in many tumor types was signally up-regulated, indicated that the CCAT2 was closely associated with risk of

several cancers [12]. Cumulative reports have demonstrated that CCAT2 played favorable role in progress and metastasis of many tumor types through multiple mechanisms [13-16]. For example, Guo et al. have demonstrated that lncRNA CCAT2 was able of enhance the migration of glioma cells through regulating the Wnt/β-catenin signaling pathway [17]. Additionally, other researchers reported that lncRNA CCAT2 promoted the migration and invasion of tumor cells though induction of epithelial-to-mesenchymal transition or regulating the pokemon expression [18,19].

There are a wide range of miRNAs are involved in the tumorigenesis and development of NSCLC [20]. miR-204, generally composed by two different mature microRNA isoforms miR-204-3p and miR-204-3p, has been demonstrated possess the suppressor role in tumorigenesis [21]. It was widely proved that the miR-204, especially the miR-204-3p, was frequently downregulated in many cancer types and loss of miR-204 expression was favorable for the growth and migration of tumor cells [22]. The miR-204 exhibited diverse functions for inhibition of tumorigenesis through target certain genes and/or signaling pathways [22]. However, the correlation between the miR-204 and development of NSCLC are not thoroughly investigated to date.

In the present study, the levels of CCAT2 in lung cancer tissues and cells were determined and compared with the corresponding normal ones. Besides, the role of CCAT2 in regulation of proliferation, invasion, migration, and drug-resistance of lung cancer were investigated as well. Additionally, the underlying correlation between the miR-204 and NSCLC and its underlying mechanisms were further thoroughly studied.

Materials And Methods

Materials

DDP was obtained from Melonepharma (Dalian, China). The cell counting kit-8 (CCK-8) was purchased from Dojindo Molecular Technologies (Gaithersburg, MD). The RPMI 1640 medium and fetal bovine serum (FBS) were obtained from Gibco (CA, USA) while the 100 U/mL penicillin/streptomycin was purchased from Sigma-Aldrich (St. Louis, MO, USA). The cell apoptosis kit was purchased from Beyotime Institute of Biotechnology (Haimen, China). The primers were obtained from Sangon Biotech (Shanghai, China) while the primary and/or second anti-bodies were purchased from BD Bioscience (San Diego, CA, USA). CCAT2, CCAT2 small interfering RNA (siRNA), negative control (NC) siRNA, and fluorescein isothiocyanate (FITC)-labeld CCAT2, si-CCAT2, and NC-siRNA were purchased from Guangzhou RiboBio Co., Ltd. (Guangzhou, China). All of the other chemicals were analytical or reagent grade.

Cell culture and animals models

Cells, including the lung cancer cell lines (H520 and A549) and normal control cell lines (BEAS2B, CCD-8L, and LL24) were obtained from the American Type Culture Collection (ATCC). The cisplatin-resistant A549/DDP cell lines were obtained from the Bank of Cancer Cell Lines of the Chinese Academy of Medical Science (Beijing, China). All cells were cultured in the RPMI 1640 containing 10% FBS and

supplemented with and 100 U/mL penicillin/streptomycin at 37℃ in a humidified incubator with 5% CO_2. The male Balb/c nude mice, age of 4-5 weeks and weight of 20 ± 2 g, were achieved from BK Lab Anima Ltd. (Shanghai, China) and raised under standard condition with free access to food and water.

Cell transfection

Transfection of cells with CCAT2, si-CCAT2, and NC-siRNA (or FITC-labeld CCAT2, si-CCAT2, and NC-siRNA) was performed using the Lipofectamine 2000 (Invitrogen, USA) in accordance with the manufacturer's guidelines. In brief, 1×10^4 A549 cells were seeded in six-well plates. After grown for 70% confluency, the plasmids containing different RNAs plus lipofectamine 2000 was added and co-incubated with cells for 6 h. Then the cell uptake efficacy and transfection efficiency was respectively determined by fluorescent analysis under a fluorescent microscopy (Leica DMI4000 B, Germany) and quantitative analysis of the CCAT2 expression by RT-qPCR assay.

Colony formation assay

5×10^3 of the transfected A549 cells were seeded into six-well plates and cultured for 10 days with the culture medium were replaced with fresh medium every two days. Then the cells in each well were stained with 0.1% crystal violet for 20 min followed by washing three times with phosphate buffer saline (PBS, pH 7.4). Finally, the colony numbers of cells were qualitatively analyzed under a invert microscopy (LSM710, Leica, Germany).

Migration and invasion assay

The lateral migration ability of A549 cells after transfection was determined by the wound-healing assay. In brief, 5×10^4 of the transfected cells were seeded in the six-well plates and allowed to culture for 24h. Then the old medium was replaced with fresh mediums and the cells were incubated until the full monolayer was formed. Subsequently, a 150 μl sterile polystyrene micropipette tip was applied to make an artificial wound of scratched cells. The scratch were photographed respectively at the 0 h and 24 h using the invert microscope.

The vertical invasion ability of A549 cells after transfection was determined by the trans-well assay. For investigation, 5×10^4 of the transfected cells in 100 μL serum-free medium were seeded in the top chamber of the 24-well trans-well while the lower chamber was filled with 600 μL medium containing 10% FBS. After incubation for 24 h, the cells invaded into the lower surface of the insert chamber were stained with 0.1% crystal followed by qualitative analysis using the invert microscope and quantitative analysis by the microplate reader (Thermo Multiskan MK3, USA).

Cell growth assay

5×10^3 of the transfected A549 cells were seeded in 96-well plates and cultured for an overnight. Then the old medium in each well of the plates was replaced with fresh culture medium and continue to

incubate for 12, 24, 48 h, respectively. To detect the cell growth rate, 10 μL of CCK-8 reagent was added and incubated with cells for 4 h followed detection at 450 nm using the microplate reader.

Additionally, to investigate whether elevation of CCAT2 expression alleviated the cytotoxicity of DDP, the transfected A549 cells were seeded as above. Then 0.5 μg/mL of DDP were added into each well and co-incubated with cells for 12, 24, 48 h, respectively. After addition of 10 μL of CCK-8 reagent and incubation for 4 h, the absorbance of the cells were detected as above.

Cell apoptosis assay

To further investigate the effect of CCAT2 on the alleviation of cytotoxicity of DDP to A549 cells, cell apoptosis assay was performed. 5×10^4 transfected A549 cells were seeded in 6-well plates and allowed to grow for overnight. Then the old medium in each well was replaced with fresh serum-free medium containing DDP (0.5 μg/mL). After incubation for 24 h, the cells in each well were harvested by centrifugation at 1000 g for 5 min. Then the apoptosis of cells was examined using the double staining (propidium iodide and annexin V) approach and determined by the FACSscan Flow Cytometer (BD PharMingen, Heidelberg, Germany).

Western blot analysis

Total proteins in the tumor tissues and cells was extracted using the TRIzol reagent (Invitrogen, Carlsbad, CA) and performed in accordance with the manufacturer's instructions. Then the concentration of protein was determined using the BCA protein assay kit (Pierce, Thermo Scientific). The tissue or cell lysis solutions were separated by the SDS-PAGE followed by transplant to the polyvinylidene difluoride (PVDF) membranes ((Millipore Corp., Billerica, MA, USA). After that, the membranes were blocked by 5% non-fat milk in TBST buffer for 1 h followed by co-incubation with various primary antibodies (1:100) including anti-P-gp, -MRP, -IGFBP2, -p-AKT/AKT, and -Bcl2 for overnight. Subsequently, peroxidase-conjugated secondary antibodies (1:1000) were introduced and co-incubated with the samples for 1 h before visualization of the signal using enhanced chemiluminescence (ECL) method using chemiscope 5600 (CLINX, Shanghai, China). The protein expression levels were normalized to that of GAPDH (Sangon Biotech, Shanghai, China) and semi-quantitative analysis was performed by densitometric scanning.

Real-Time Quantitative PCR (RT-qPCR)

The RNA in tissues and cells was obtained as above. After that, the PrimeScript RT Master Mix (Takara, Tokyo, Japan) was applied to conduct the cDNA followed by analysis of the RT-qPCR using the SYBR Green PCR master mix (Takara, Tokyo, Japan). The primer sequences were as follows: CCAT2, forward, GGCCTGTAGGAAGAGTCAAATAG, and reverse, AGGTCAGGAATCAGGAGACA; si-CCAT2, forward, GATCC GTGCAACTCTGCAATTTAACACTTCCTGTCAGATGTTAAATTGCAGAGTTGCACTTTTTG, and reverse, AATTCAAAAAGTGCAACTCTGCAATTTAACA TCTGACAGGAAGTGTTAAATTGCAGAGTTGCACG; NC siRNA, forward, GATCCGCCACTTTGAAGAACCCAATCCTTCCTGTCAGGATTGGGTTCTTCAAAGTGGCTTTTTG, and reverse, AATTCAAAAAGCCACTTTGAAGAACCCAATC

TCTGACAGGAAGGATTGGGTTCTTCAAAGTGGCG; AKT forward, GGACAACCGCCATCCAGACT, and reverse, GCCAGGGACACCTCCATCTC; BCl_2 forward, TTCTTTGAGTTCGGTGGGGTC, and reverse, TGCATATTTGTTTGGGGCAGG; IGFBP2F forward, GGGACTGCTTTCCAATAG, and reverse, TTACAGTCTTTGGTCTCGG; GAPDH, forward, CGGAGTCAACG GATTTGGTCGTA, and reverse, AGCCTTCTCCATGGTGGTGAAGAC. The protein expression levels were normalized to that of GAPDH.

In vivo tumor growth and progression assay

The A549 cancer-bearing mice models were established using the subcutaneous transplantation approach. In brief, 2×10^6 of the transfected A549 cells in 100 μL RPMI-1640 (FBS free) were subcutaneously injected into the right flanks of mice. Then the mice were grouped (*n=10*) according to the injected cells: Control group (non-transfected A549 cells), NC siRNA group (NC siRNA transfected A549 cells), CCAT2 group (CCAT2 transfected A549 cells), and si-CCAT2 group (si-CCAT2 transfected A549 cells). All mice from each group were raised under the standard condition with free access to food and water. For tumor growth observation, the tumor volume changes of mice in each group were carefully calculated every three days using the formula: Volume = $0.5 \times \text{length} \times (\text{width})^2$. For survival investigation, the deaths in each group were carefully recorded for finally Kaplan-Meier curve analysis. Besides above, the effect of CCAT2 regulating the anti-tumor effect of DDP was further investigated *in vivo*. Tumor-bearing mice were established and grouped (*n=10*) as above. Then the mice in each group was treated with DDP (5mg/kg) *via* tail intravenous injection. The treatment was done every two days in a week (a total of three times). Then the tumor volume change and survival time of each mice were carefully calculated and recorded. At the end of *in vivo* experiments, all tumor tissues were obtained for further analysis after the alive mice were euthanized.

Immunohistochemistry (IHC) study and TUNEL assay

The obtained tumor tissues were prepared for 5 μm slides followed by incubated with primary antibodies (anti-miR-204-3p, 1:100) for an overnight. Then the primary antibodies were withdrawn and replaced with the streptavidin peroxidase-conjugated second-antibodies (1:1000). After incubation for 1h, the results were obtained using the invert microscope. The Tdt-mediated dUTP nick-end labeling (TUNEL) assay was performed according to the protocol of NeuroTACS II In Situ Apoptosis Detection Kit. The tumor slide samples were counterstained with hematoxylin while positive signals were developed by diaminobenzidine (DAB). Finally, the results were achieved by the invert microscope.

Statistical analysis

The data in the present study were expressed as the means ± SD. The statistical analyses were performed using the GraphPad Prism 7.0 version program. The Student's t-test was applied to evaluate the difference between two means and the comparison between more than two groups was carried out by one-way ANOVA. The experiments performed here were repeated at least three times and the statistical significance was defined as $P<0.05$.

Results

High level of CCAT2 in non-small lung cancer cells and tissues resulted in rapid tumor growth and poor survival

The expressions of CCAT2 in non-small lung cancer cells and tissues were firstly investigated through the RT-qPCR experiments and compared with the corresponding normal cells or tissues. As shown in Figure 1A, obvious higher signal of CCAT2 was detected in the NSCLC cell lines compared with the normal cell lines. Moreover, it was displayed that the signal of CCAT2 in the drug-resistant cells (A549/DDP) was markedly stronger than that in the non-resistant A549 cells. It might indicated that CCAT2 played significant role in the development of drug-resistant NSCLC. The levels of CCAT2 expression in NSCLC tissues and the adjacent non-carcinoma tissues were further quantitatively investigated. Results showed that aberrant high expression of CCAT2 was detected in NSCLC tissues while not the non-tumor tissues (Figure 1B).

Subsequently, the effect of CCAT2 on promotion of the growth and progress of NSCLC was determined *in vivo*. As shown in Figure 1C, the mice bearing with A549 cancer (relative low CCAT2 expression) exhibited an obvious slower tumor growth rate than the mice bearing with A549/DDP (relative high CCAT2 expression). Additionally, the A549/DDP cancer-bearing mice have a more poor survival than the A549 cancer-bearing mice (Figure 1D). Given these results together, it was suggested that overexpression of CCAT2 in NSCLC contribute to rapid tumor growth and poor survival.

Confirmation of cell transfection

As shown in Figure 2A, compared with the non-transfected control cells with negligible signal, obvious higher fluorescent intensity was observed in the RNA transfected cells. Moreover, there was no significant difference was observed between the NC siRNA, CCAT2, and si-CCAT2 group, suggested similar amount of plasmids was uptake by A549 cells between the three groups. Subsequently, the cell transfection was confirmed by quantitative analysis of the expression of CCAT2 using the RT-qPCR assay. As shown in Figure 2B, obvious higher expression of CCAT2 was detected in the CCAT2-transfected cells than the control and NC siRNA group. In contrast, significant lower signal of CCAT2 was observed in the si-CCAT2 group. These results demonstrated that the A549 cells were successfully transfected with various RNAs.

Up-regulation of CCAT2 dramatically enhanced the proliferation, migration and invasion of A549 cells

As shown in Figure 2C, results of the colony assay revealed that up-regulation of the CCAT2 level in A549 cells dramatically promoted the proliferation rate. In contrast, after knockdown of the CCAT2 expression in A549 cells, the proliferation rate was markedly decreased. The lateral migration ability of A549 cells after various transfection was subsequently evaluated using the wound healing assay. As shown in Figure 2D, it was revealed that faster closing of scratch wounds was observed in the cells overexpressed with CCAT2 compared with the CCAT2 negative cells. However, the migration speed of cells transfected with si-CCAT2 was dramatically restricted. The vertical invasion was further investigated using the trans-

well experiments. As displayed in Figure 2E, overexpression of CCAT2 significantly improved the invasion ability of A549 cells, with more amount of crystal violet was obtained in the CCTA2 group than others. Finally, cell growth rate of A549 cells post different transfection was evaluated by the CCK-8 assay. As demonstrated in Figure 2F, increase the CCAT2 levels in A549 cells contributed to a dramatic increased cell growth rate. However, the growth of A549 cells could be markedly inhibited by transfection with si-CCAT2. The results above together indicated that the CCAT2 has played essential role in the proliferation, migration and invasion of NSCLC cells.

CCAT2 significantly down-regulated the sensitivity of A549 cells to the treatment of DDP

As shown in Figure 3A, it was revealed that increase the level of CCAT2 in A549 cells significantly down-regulated the ability of DDP to inhibit cell growth. In contrast, the cells transfected with si-CCAT2 exhibited obvious lower growth rate than other groups. Apoptosis rate of the transfected A549 cells after treatment of DDP was further determined. As shown in Figure 3B, there was no significant difference between the group of DPP and NC siRNA + DDP. However, the apoptosis rate of cells in the group of CCAT2 + DDP was signally decreased while that in the group of si-CCAT2 + DDP was dramatically elevated. Semi-quantitative analysis revealed that the medium percentage of early and late apoptosis for each group was 8.16 ± 3.6% for DDP, 7.63 ± 1.8% for NC siRNA + DDP, 4.51 ± 1.7% for CCAT2 + DDP, and 20.37 ± 2.3% for siCCAT2 + DDP, respectively (Figure 3C). To further that CCAT2 was able of inducing drug-resistance of A549 cells, the drug-resistant related proteins, P-glycoprotein (P-gp) and multidrug resistance related protein (MRP), were respectively determined by Western-blot and RT-qPCR assay after various treatments. As demonstrated in Figure 3D, the levels of P-gp and MRP in the group of CCAT2 + DDP was significantly higher than others. On the contrary, expressions of P-gp and MRP in the cells treated by si-CCAT2 + DDP was the lowest in all groups. Such results were further confirmed by the semi-quantitative analysis and quantitative determination thorough the RT-qPCR experiment (Figure 3E).

CCAT2 enhanced the proliferation, migration, invasion and drug-resistances of A549 cells by suppress the miR-204-3p expression

Western-blot analysis revealed that transfection with A549 cells with CCAT2 signally down-regulated the expression of miR-204-3p. In contrast, treating cells with si-CCAT2 dramatically increased the level of miR-204-3p in A549 cells (Figure 4A). Further quantitative investigation by RT-qPCR confirmed that the level of miR-204-3p in the CCAT2 transfected A549 cells was nearly three times lower than that in the Control and/or NC siRNA group (Figure 4B). Interestingly, after transfection with the A549 cells with miR-204-3p, the levels of CCAT2 was signally down-regulated (Figure 4C). Therefore, the correlation analysis was further performed. Results shown in Figure 4D exhibited that the expression of miR-204-3p was negatively correlated with the CCAT2 expression. These results together suggested that the CCAT2 promoted the progress of A549 thorough inhibition of the miR-204-3p.

Up-regulation of CCAT2 activated the miR-204-3p-suppresed IGFBP2/AKT/Bcl2 pathway

The downstream genes of miR-204-3p was subsequently investigated. As shown in Figure 5, the cells transfected with CCAT2 exhibited the highest levels of IGFBP2, p-AKT/AKT, and BCl_2 in all groups. In contrast, after transfection of the lung cancer cells with miR-204-3p, the expression of IGFBP2, p-AKT/AKT, and BCl_2 was dramatically decreased. Additionally, there was no significant difference was observed between the group of non-transfected cells and transfected with CCAT2 plus miR-204-3p. These results demonstrated that increase the CCAT2 expression was able of activating the miR-204-3p-suppresed IGFBP2/AKT/Bcl2 pathway.

CCAT2 promoted the progress and drug-resistance of A549 tumor *in vivo* through activation of the miR-204-3p suppressed IGFBP2/AKT/Bcl2 pathway

In vivo tumor growth assay (Figure 6A and 6B) revealed that the mice transplanted with the CCAT2 transfected cells exhibited the fastest tumor growth rate. In contrast, the tumors in the group of si-CCAT2 displayed the slowest growth rate. RT-qPCR analysis of the drug-resistant related proteins showed that the overexpression of CCAT2 signally increased the levels of P-gp and MRP in the tumor tissues (Figure 6C). Results of IHC analysis displayed that the tumor tissues in the group of CCAT2 have the lowest level of miR-204-3p (Figure 6D and 6E), which resulted in the highest levels of IGFBP2, p-AKT/AKT, and BCl_2 (Figure 6F). However, the expression of miR-204-3P in A549 cells could be signally activated by treating with si-CCAT2, and in turn signally down-regulated the activity of IGFBP2/AKT/Bcl_2 pathway.

Further experiments were performed with the presence of DDP. As shown in Figure 6G and 6H, tumors in the group of CCAT2+DDP exhibited the fastest deteriorative speed and the highest tumor weight, which similar to the above results. Additionally, results of the survival time revealed that the mice in the group of CCAT2+DDP achieved the shortest medium survival time while that of the si-CCAT2+DDP group achieved the longest medium survival time (Figure 6I). TUNEL evaluation in Figure 5J and 5K exhibited that the CCAT2 could dramatically down-regulated the cytotoxicity of DDP to A549 tumors. However, down-regulation of the CCAT2 level significantly enhanced the tumor inhibition effect of DDP. Taking these results together, it could be concluded that the CCAT2 enhanced the progress of A549 tumor *via* targeting the miR-204-3p and induced the drug-resistance.

Discussion

Previous studies have demonstrated that lncRNAs cloud be acted as the novel tumor biomarkers so that provide a novel approach for early diagnosis and treatment of a wide range of malignant cancers [23-25]. As an lncRNA that specifically expressed in many cancer types, CCAT2 was proved to be able of accelerated the deterioration of tumors through promotion of the growth and metastasis of tumor tissues and induce chromosomal instability [26]. In the present study, it was revealed that the NSCLC tissues and cells were detected with high level of CCAT2. In contrast, significantly lower signal of CCAT2 was observed in the normal adjacent tissues and various lung cancer tissues. Additionally, the expression of CCAT2 in the cisplatin-resistant lung cancer cells was obvious higher than the non-resistant ones, indicated that CCAT2 might play significant role in the development of drug-resistance for NSCLC.

It was previously revealed that the CCAT2 played significant role in a variety of biological regulation processes, such as cell proliferation, invasion, and migration [14,15]. Aberrant expression of CCAT2 in tumor tissues and cells was supposed to be the favorable factor that leaded to enhanced growth and metastasis of tumors and proliferation of cancer cells [26]. Our study confirmed that overexpression of CCAT2 dramatically promoted the proliferation and migration rate of lung cancer cells, whereas knockdown of CCAT2 expression resulted in obvious decreased growth rate. Additionally, high level of CCAT2 in NSCLC cells signally contributed to the improvement of invasion ability of NSCLC cells. Moreover, up-regulation of CCAT2 level contributed to the rapidest deteriorate rate of tumor-bearing mice further confirmed the positive role of CCAT2 in the progress of NSCLC

Treatment of lung cancer, especially the NSCLC, always seriously obstructed by the limited strategies, rapid deteriorate rate, and the development of drug-resistance during the treatment late [27]. As the platinum-containing anticancer drug, cisplatin has been recommend for the therapy of multi types of malignant cancer [28]. Although the cisplatin was demonstrated to be one of the most potent chemotherapeutic agent, the development of cisplatin resistance dramatically weaken the treatment efficacy of cancer.29 Multiple mechanisms may resulted the cisplatin resistance, such as excessive drug accumulation, inactivation of agents, and enhanced repair of DNA damage [29,30]. In our study, we demonstrated that up-regulation of CCAT2 level significantly decreased the inhibition effect of DDP on the growth and inducing apoptosis of NSCLC cells and tissues. On the contrary, knockdown of the CCAT2 expression was favorable for the improvement of tumor inhibition effect of DDP. Molecule detection revealed that increase the level of CCAT2 in NSCLC cells and tissues contributed to significantly elevated expression P-gp and MRP. Such results indicated that the CCAT2 decreased the sensitivity of NSCLC to the treatment of DDP through up-regulation of drug-resistance related proteins.

The miR-204-3p has been found to be deregulated in several tumors, such as hepatocellular carcinoma, glioma, and breast cancer [31,32], and is closely related with clear cell renal cell carcinoma and upper tract urothelial carcinomas [33]. However, whether there was relationship between the CCAT2 and miR-204-3p remains unclear. In the present study, it was revealed that increase the level of CCAT2 dramatically decreased the miR-204-3p expression in NSCLC cells and tissues. Interestingly, up-regulation of the miR-204-3p level signally down-regulated the activation of CCAT2 in NSCLC cells and tissues. Such negative correlation between the CCAT2 and miR-204-3p suggested that the CCAT2 regulated proliferation, migration, and growth of NSCLC through targeting the miR-204-3p.

The miRNAs regulates multiple cellular process mainly through regulates the expression of its targeted genes and the downstream signaling pathways [18]. There are a wide array of signaling are involved in the tumorigenesis and progress of cancers. Among these, the IGF signaling pathway plays essential role in the embryonic development and also the carcinogenesis [34,35]. It was found that the IGF-binding protein (IGFBP) superfamily have the inhibitory effects on the activation of IGFs [36]. Of great importance, increasing evidences demonstrated that IGFBP played favorable role in the progress of many carcinogenesis, with aberrant expression of IGFBP and its downstream genes, including p-AKT/AKT and BCl2, signally promoted cancer cell survival and migration [32]. Whether the miR-204-3p inhibited the

growth of NSCLC through targeting silence the bioactivity of IGFBP2/AKT/Bcl2 signaling is not clear. In our study, it was revealed that down-regulation of miR-204-3p by transfection with CCAT2 signally activated the levels of IGFBP2, p-AKT/AKT, and BCl2 in lung cancer cells and/or tissues. In contrast, up-regulation of miR-204-3p resulted in dramatically decreased bioactivity of IGFBP2/AKT/Bcl2 pathway and in turn contributed to a relative ideal inhibition effect on tumor growth. Taking together, the present study demonstrated that CCAT2 promoted progress of non-small lung cancer via activating the miR-204-3p-suppresed IGFBP2/AKT/Bcl2 pathway.

Conclusion

In summary, our study confirmed a higher levels of CCAT2 was detected in NSCLC cell lines and tissues. Subsequent experiments demonstrated that up-regulation of CCAT2 resulted in rapid proliferation, migration, and invasion of lung cancer cells. Moreover, it was also revealed that overexpression of CCAT2 contributed to the development of drug-resistance by up-regulation of drug-resistant related proteins. Further mechanisms investigation demonstrated that the CCAT2 promoted the progress of NSCLC through suppression of the miR-204-3p levels and finally activation of the IGFBP2/AKT/Bcl2 pathway.

Declarations

Authors' contributions

Zheng Wang was responsible for the guarantor of integrity of the entire study and preparation, editing, and review of the manuscript. Rongjie Yang and Yu Liu were respectively involved in the definition of intellectual content and literature research. Yangfeng Hang responsible for the study design, data acquisition and analysis.

Funding

This study was supported by the Natural Science Foundation of Liaoning Province, China (grant no. 201602449).

Acknowledgements

We thank the supports from all participants.

Availability of data and materials

The data are available from the authors upon request.

Ethics approval and consent to participate

The experimental protocol related animals in the present study was approved by the Animal Experimentation Ethics Committee of Cancer Hospital of China Medical University.

Consent for publication

Not applicable

Competing interests

The authors declare that they have no competing interests.

Abbreviations

NSCLC, non-small cell lung cancer; CCAT2, colon cancer-associated transcript 2; IGFBP, IGF-binding protein; DDP, cisplatin; ncRNA, non-coding RNA; LncRNA, long non-coding RNA; CCK-8, cell counting kit-8; RT-qPCR, real-Time Quantitative PCR; IHC, immunohistochemistry; P-gp, p-glycoprotein; MRP, multidrug resistance related protein; IGF, insulin-like growth factor.

References

1. Torre LA, Bray F, Siegel RL, Ferlay J, Lortet-Tieulent J, Jemal A. Global cancer statistics, 2012. CA Cancer J Clin 2015;65:87-108.
2. Prokop M. Lung cancer screening: the radiologist's perspective. Semin Respir Crit Care Med 2014;35:91-98.
3. Wang Y, Shen Y, Sun X, Hong TL, Huang LS, Zhong M. Prognostic roles of the expression of sphingosine-1-phosphate metabolism enzymes in non-small cell lung cancer. Transl Lung Cancer Res 2019;8:674-681.
4. Miura N, Kohno M, Ito K, Senba M, Kajiwara K, Hamaguchi N, Makino H, Kanematsu T, Okamoto T, Yokoyama H. Lung cancer surgery in patients aged 80 years or older: an analysis of risk factors, morbidity, and mortality. Gen Thorac Cardiovasc Surg 2015;63:401-405.
5. Fan Y, Huang Z, Fang L, Miu L, Lin N, Gong L, Yu H, Yang H, Mao W. Chemotherapy and EGFR tyrosine kinase inhibitors for treatment of brain metastases from non-small-cell lung cancer: survival analysis in 210 patients. Onco Targets Ther 2013;6:1789-1803.
6. Simmons CP, Koinis F, Fallon MT, Fearon KC, Bowden J, Solheim TS, Gronberg BH, McMillan DC, Gioulbasanis I, Laird BJ. Prognosis in advanced lung cancer--A prospective study examining key clinicopathological factors. Lung Cancer 2015;88:304-309.
7. MacDonagh L, Gray SG, Finn SP, Cuffe S, O'Byrne KJ, Barr MP. The emerging role of microRNAs in resistance to lung cancer treatments. Cancer Treat Rev 2015;41:160-169.
8. Gelvan A, Risum S, Langer SW. Incidence and survival from lung cancer in Greenland is comparable to survival in the Nordic countries. Dan Med J 2015;62:A5033.
9. Zhou ZJ, Zhan P, Song Y. PD-L1 over-expression and survival in patients with non-small cell lung cancer: a meta-analysis. Transl Lung Cancer Res 2015;4:203-208.

10. Cloutier SC, Wang S, Ma WK, Al Husini N, Dhoondia Z, Ansari A, Pascuzzi PE, Tran EJ. Regulated Formation of lncRNA-DNA Hybrids Enables Faster Transcriptional Induction and Environmental Adaptation. Mol Cell 2016;61(3):393-404.
11. Li H, Han Q, Chen Y, Chen X, Ma R, Chang Q, Yin D. Upregulation of the long non-coding RNA FOXD2-AS1 is correlated with tumor progression and metastasis in papillary thyroid cancer. Am J Transl Res 2019;11(9):5457-5471.
12. Ling H, Spizzo R, Atlasi Y, Ito S, Iguchi T, Sugiyama M, Nakashima Y, Ohgaki K, Saeki H, Mimori K, Maehara Y. CCAT2, a novel noncoding RNA mapping to 8q24, underlies metastatic progression and chromosomal instability in colon cancer. Genome Res 2013;23(9):1446-1461.
13. Zhou N, Si Z, Li T, Chen G, Zhang Z, Qi H. Long non-coding RNA CCAT2 functions as an oncogene in hepatocellular carcinoma, regulating cellular proliferation, migration and apoptosis. Oncol Lett 2016;12(1):132-138.
14. Wang CY, Hua L, Yao KH, Chen JT, Zhang JJ, Hu JH. Long non-coding RNA CCAT2 is up-regulated in gastric cancer and associated with poor prognosis. Int J Clin Exp Pathol 2015;8(1):779-785.
15. Zhang X, Xu Y, He C, Guo X, Zhang J, He C, Zhang L, Kong M, Chen B, Zhu C. Elevated expression of CCAT2 is associated with poor prognosis in esophageal squamous cell carcinoma. J Surg Oncol 2015;111(7):834-839.
16. Zeng J, Du T, Song Y, Gao Y, Li F, Wu R, Chen Y, Li W, Zhou H, Yang Y, Pei Z. Knockdown of Long Noncoding RNA CCAT2 Inhibits Cellular Proliferation, Invasion, and Epithelial-Mesenchymal Transition in Glioma Cells. Oncol Res 2017;25(6):913-921.
17. Guo H, Hu G, Yang Q, Zhang P, Kuang W, Zhu X, Wu L. Knockdown of long non-coding RNA CCAT2 suppressed proliferation and migration of glioma cells. Oncotarget 2016;7(49):81806-81814.
18. Xu Y, Yao Y, Qin W, Zhong X, Jiang X, Cui Y. Long Non-Coding RNA CCAT2 Promotes Cholangiocarcinoma Cells Migration and Invasion by Induction of Epithelial-To-Mesenchymal Transition. Biomed Pharmacother 2018;99:121-127.
19. Zhao Z, Wang J, Wang S, Chang H, Zhang T, Qu J. LncRNA CCAT2 promotes tumorigenesis by over-expressed Pokemon in non-small cell lung cancer. Biomed Pharmacother 2017;87:692-697.
20. Wang H, Wu S, Zhao L, Zhao J, Liu J, Wang Z. Clinical use of microRNAs as potential non-invasive biomarkers for detecting non-small cell lung cancer: a meta-analysis. Respirology 2015;20:56-65.
21. Imam JS, Plyler JR, Bansal H, Prajapati S, Bansal S, Rebeles J, Chen HI, Chang YF, Panneerdoss S, Zoghi B, Buddavarapu KC, Broaddus R, Hornsby P, Tomlinson G, Dome J, Vadlamudi RK, Pertsemlidis A, Chen Y, Rao MK. Genomic loss of tumor suppressor miRNA-204 promotes cancer cell migration and invasion by activating AKT/mTOR/Rac1 signaling and actin reorganization. PLoS One 2012;7:e52397.
22. Xia Z, Liu F, Zhang J, Liu L. Decreased Expression of MiRNA-204-5p Contributes to Glioma Progression and Promotes Glioma Cell Growth, Migration and Invasion. PLoS One 2015;10:e0132399.

23. Kwok ZH, Tay Y. Long noncoding RNAs: lincs between human health and disease. Biochem Soc Trans 2017;45:805-812.
24. Ma DD, Yuan LL, Lin LQ. LncRNA HOTAIR contributes to the tumorigenesis of nasopharyngeal carcinoma via up-regulating FASN. Eur Rev Med Pharmacol Sci 2017;21:5143-5152.
25. Das R, Feng FY, Selth LA. Long non-coding RNAs in prostate cancer: Biological and clinical implications. Mol Cell Endocrinol 2019;480:142-152.
26. Ling H, Spizzo R, Atlasi Y, Zheng Z, Bai W, Duan Y, Cheng S, Wang J, Liu X, Zhang G. CCAT2, a novel noncoding RNA mapping to 8q24, underlies metastatic progression and chromosomal instability in colon cancer. Genome Res 2013;23:1446-1461.
27. Czyżykowski R, Połowinczak-Przybyłek J, Potemski P. Nicotine-induced resistance of non-small cell lung cancer to treatment–possible mechanisms. Postepy Hig Med Dosw (Online) 2016;70:186-193.
28. Lange J, Audebert HJ, Endres M, Rocco A. Cisplatin-related Cerebral Infarction in Testicular Germ Cell Cancer: Short Report of Three Cases and P in testicular germ cell cancer: Short report of three cases and pathomechanism. Clin Neurol Neurosurg 2017;152:76-77.
29. Rose MC, Kostyanovskaya E, Huang RS. Pharmacogenomics of cisplatin sensitivity in non-small cell lung cancer. Genomics Proteomics Bioinformatics 2014;12:198-209.
30. Li Y, Jiang W, Hu Y, Da Z, Zeng C, Tu M, Deng Z, Xiao W. MicroRNA-199a-5p inhibits cisplatin-induced drug resistance via inhibition of autophagy in osteosarcoma cells. Oncol Lett 2016;12:4203-4208.
31. Cui ZH, Shen SQ, Chen ZB, Hu C. Growth inhibition of hepatocellular carcinoma tumor endothelial cells by miR-204-3p and underlying mechanism. World J Gastroenterol 2014;20:5493-5504.
32. Chen PH, Chang CK, Shih CM, Cheng CH, Lin CW, Lee CC, Liu AJ, Ho KH, Chen KC. The miR-204-3p-targeted IGFBP2 pathway is involved in xanthohumol-induced glioma cell apoptotic death. Neuropharmacology 2016;110:362-375.
33. Zaravinos A, Lambrou GL, Mourmouras N, Katafygiotis P, Papagregoriou G, Giannikou K, Delakas D, Deltas C. New miRNA profiles accurately distinguish renal cell carcinomas and upper tract urothelial carcinomas from the normal kidney. PLoS One 2014;9:e91646.
34. Le Roith D. Seminars in medicine of the Beth Israel Deaconess Medical Center. Insulin-like growth factors. N Engl J Med 1997;336:633-640.
35. Samani AA, Yakar S, LeRoith D, Brodt P. The role of the IGF system in cancer growth and metastasis: overview and recent insights. Endocr Rev 2007;28:20-47.
36. Guha N, Nevitt SP, Francis M, Woodland JA, Böhning D, Sönksen PH, Holt RI. The Effects of Recombinant Human Insulin-Like Growth Factor-I/Insulin-Like Growth Factor Binding Protein-3 Administration on Body Composition and Physical Fitness in Recreational Athletes. J Clin Endocrinol Metab 2015;100:3126-3131.

Figures

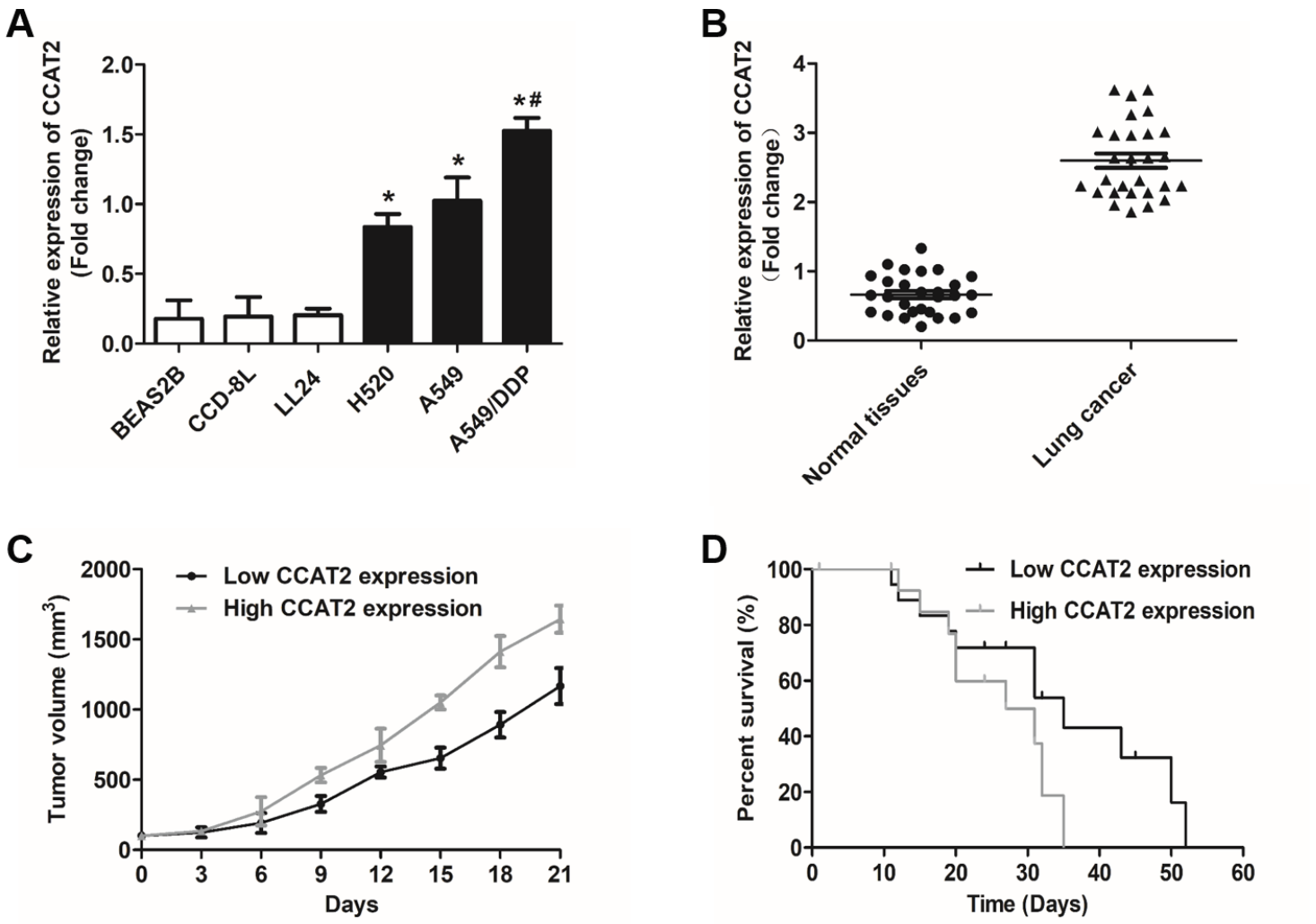


Figure 1

High level of CCAT2 in non-small lung cancer cells and tissues resulted in rapid tumor growth and poor survival. (A) The levels of CCAT2 in various lung cancer cells and compared with a series of normal cells determined by RT-qPCR assay. (B) Quantitative evaluation of the CCAT2 expression in NSCLC tissues and compared with the adjacent normal tissues by RT-qPCR assay. (C) The changes of tumor volumes in the mice subcutaneously transplanted with high and low CCAT2 expression cancer cells (A549/DDP). (D) The medium survival of time of mice bearing the high and low CCAT2 expression tumors investigated by the Kaplan-Meier curve. *P<0.05, significantly higher than the normal cells or adjacent non-tumor tissues. #P<0.05, significantly higher than the non-resistant A549 cells.

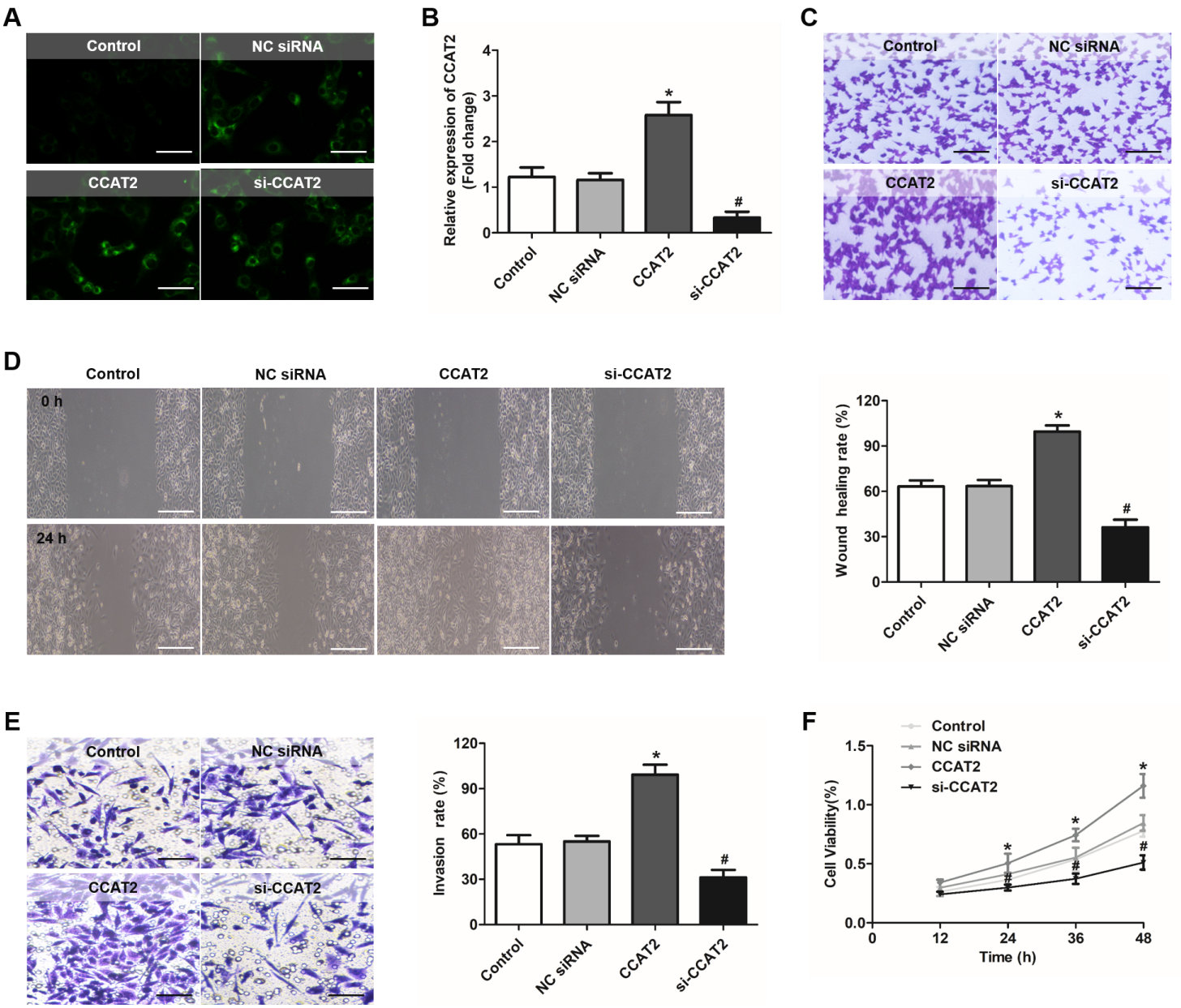


Figure 2

Up-regulation of CCAT2 dramatically enhanced the proliferation, migration and invasion of A549 cells. (A) Fluorescent intensity of cells after respectively transfected with FITC-labeled CCAT2, si-CCAT2, and NC siRNA, determined by the Fluorescence Inversion Microscope System. (B) Quantitatively analysis of the CCAT2 expression in cells after respectively transfected with CCAT2, si-CCAT2, and NC siRNA by RT-qPCR experiments. (C) Proliferation of cells post different treatments investigated by the colony formation assay. (D) Migration ability of cells after transfected with different RNAs evaluated by the wound healing assay. (E) Invasion ability of cells after transfected with different RNAs examined by the trans-well assay. (F) Cell viability of cells at different time points post treatments with NC siRNA, CCAT2, and si-CCAT2, respectively. *P<0.05, #P<0.05 significantly different from the control group and NC siRNA. The bar is 100 μm.

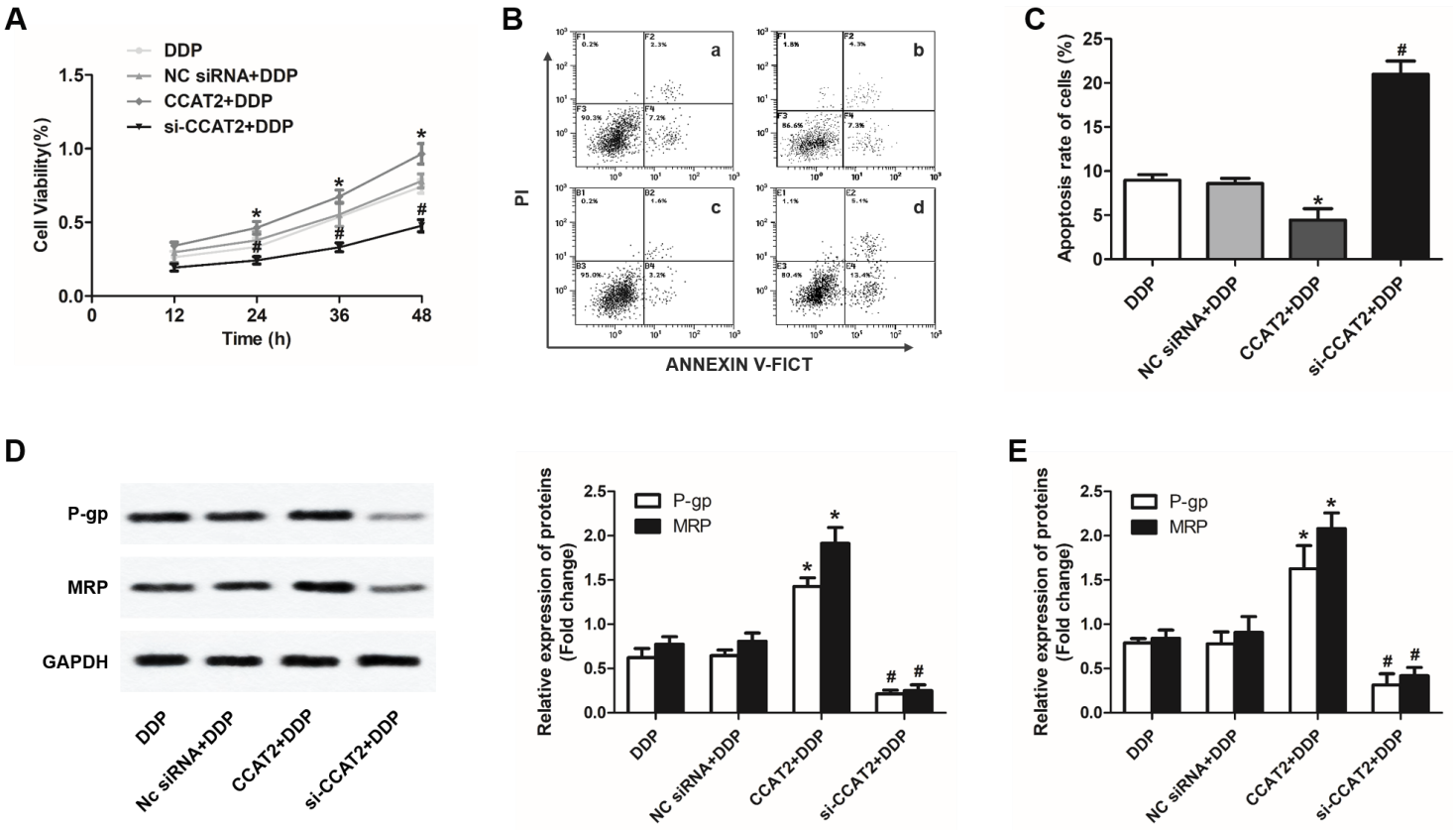


Figure 3

Aberrant overexpression of CCAT2 significantly decreased the sensitivity of A549 cells to the treatment of DDP. (A) Cell viability of A549 cells after treated with various strategies determined by the CCK-8 assay. (B) Flow cytometry analysis of the apoptosis rate of A549 cells in the group of DDP (a), NC siRNA + DDP (b), CCAT2 + DDP (c), si-CCAT2 + DDP (d). (C) Semi-quantitative analysis of the apoptosis rate of A549 cells post the flow cytometry experiments. (D) Qualitative and semi-quantitative evaluation of the levels of P-gp and MRP in A549 cells post different treatments determined by Western-blot assay. (E) Quantitative investigation of the P-gp and MRP expressions in A549 cells after various treatments by RT-qPCR assay. *P<0.05, #P<0.05 significantly different from the cells treated with DDP and NC siRNA + DDP.

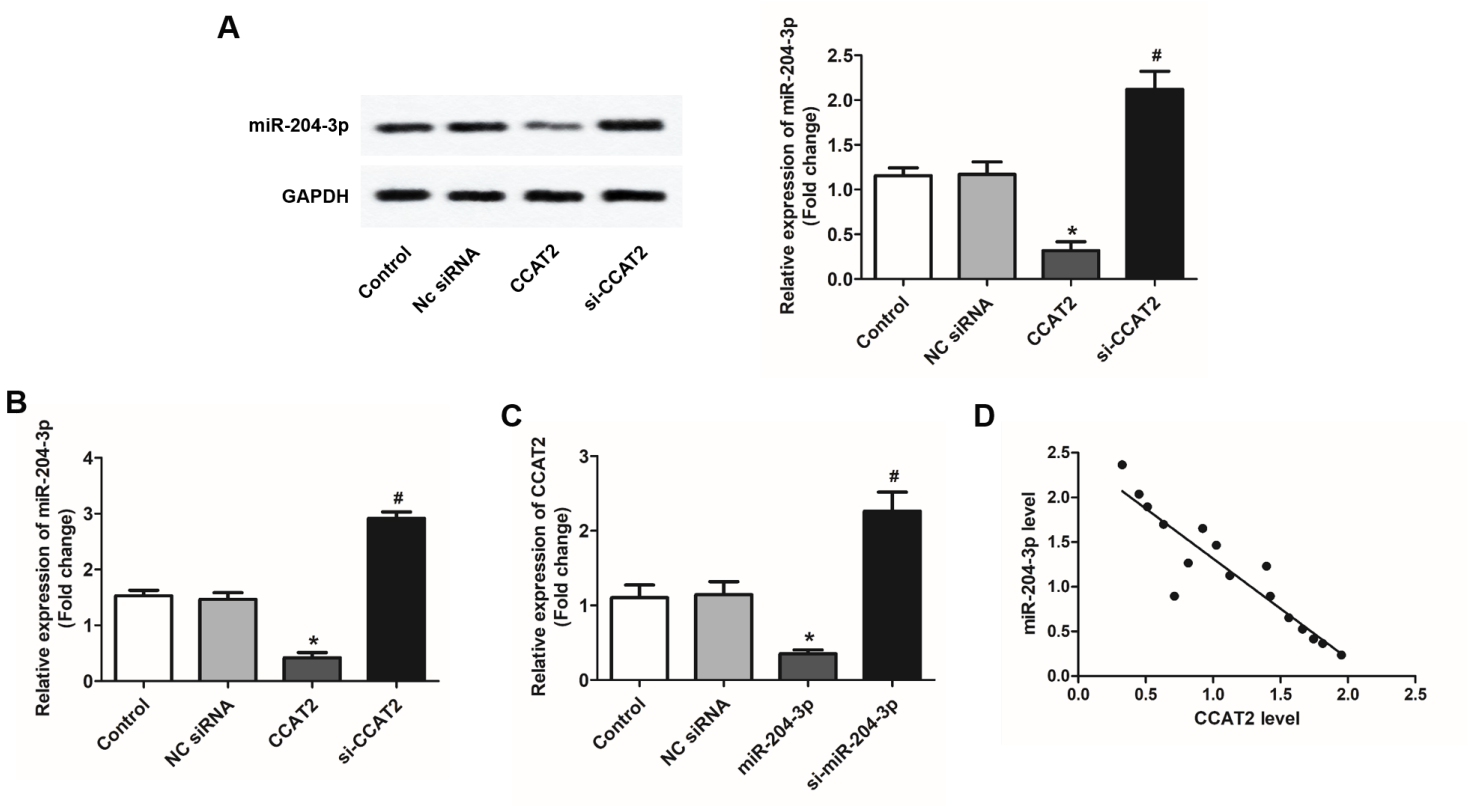


Figure 4

Increase the level of CCAT2 dramatically down-regulated the expression of miR-204-3p. (A) Qualitative analysis and semi-quantitative evaluation of the level of miR-204-3p in A549 cells after various treatments determined by Western-blot assay. (B) Quantitative investigation of the expression of miR-204-3p in A549 cells after different transfection examined by RT-qPCR assays. (C) RT-qPCR analysis of the expression of CCAT2 in A549 cells after respectively transfected with NC siRNA, miR-204-3p, and si-miR-204-3p. (D) Investigation of the correlation between the expression of miR-204-3p and CCAT2. *P<0.05, #P<0.05 significantly different from the control group and cells treated with NC siRNA.

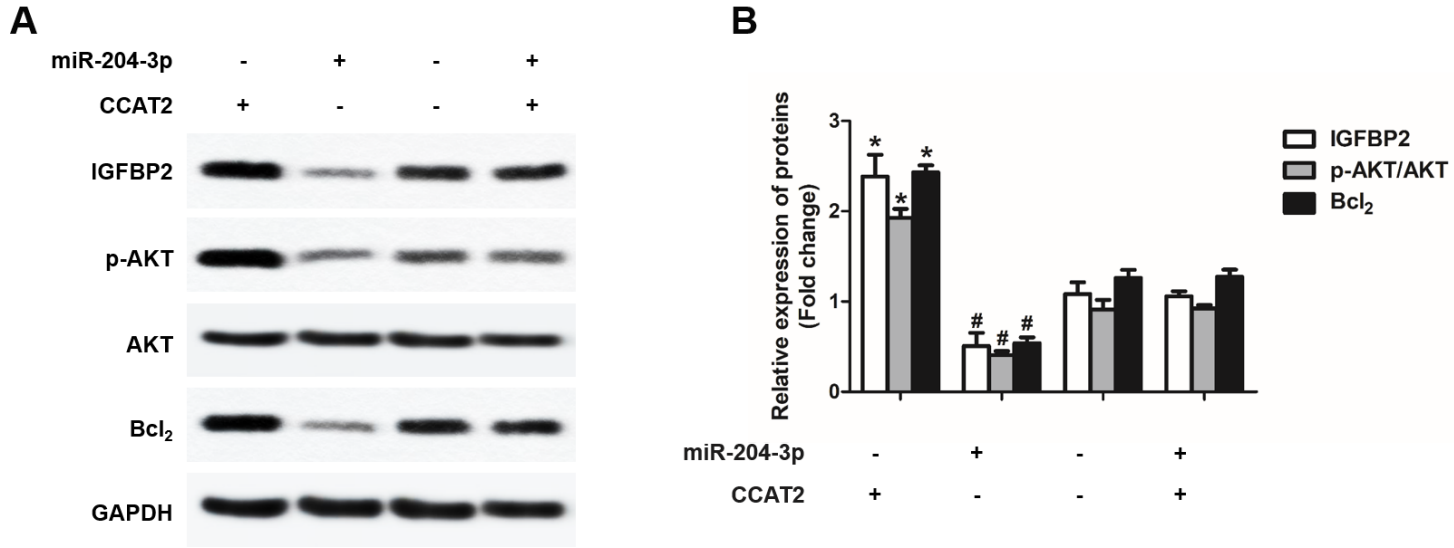


Figure 5

Increase the CCAT2 level signally inhibited the miR-204-3p mediated IGFBP2/AKT/Bcl2 pathway. Qualitative (A) and semi-quantitative (B) analysis of the downstream genes of miR-204-3p, including the IGFBP2, p-AKT/AKT, and BCl2, after different treatments. *P<0.05, #P<0.05 significantly different from the cells non-transfected with miR-204-3p or CCAT2 or simultaneously transfected with miR-204-3p and CCAT2.

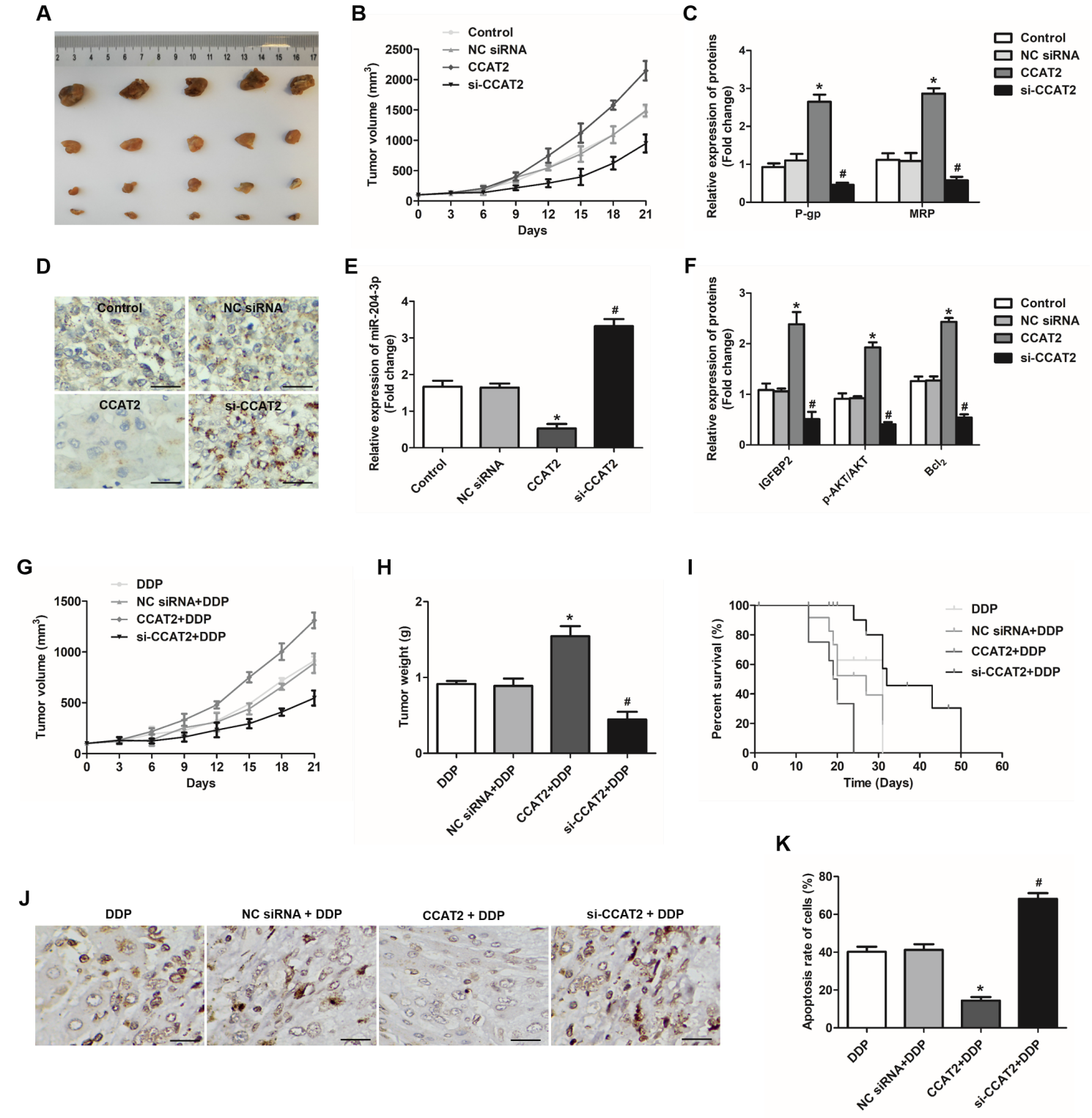


Figure 6

Overexpression of CCAT2 promoted the progress of A549 tumor thorough inhibition the miR-204-3p and activation of the IGFBP2/AKT/Bcl2 pathway. Tumor images (A) and tumor volumes changes (B) of mice after respectively treated by NC siRNA, CCAT2, and si-CCAT2. The mice transplanted with non-gene transfected A549 cells used as the control. (C) RT-qPCR analysis of the expression of P-gp and MRP in tumor tissues at the end of tumor growth experiments. Qualitative (D) and semi-quantitative (E) evaluation of the miR-204-3p level in tumor tissues by IHC analysis. (F) Quantitative analysis of the expression of IGFBP2, p-AKT/AKT, and BCl2 in tumor tissues. Tumor volumes changes (G), tumor weight (H), and percent survival time (I) of mice after respectively treated by DDP, NC siRNA + DDP, CCAT2 + DDP, and si-CCAT2 + DDP. Qualitative (J) and semi-quantitative (K) evaluation of the cytotoxicity of DDP to tumor tissues by TUNEL assay. *P<0.05, #P<0.05 significantly different from the control and NC siRNA or DDP and NC siRNA + DDP. The bar is 100 μm.